Shelf Break Momentum Transport by Internal Waves Generated by Along-Slope Currents over Topography

S.A. Thorpe, D. Jiang, and J.M. Keen

Department of Oceanography, The University, Southampton, SO9 5NH, UK

Abstract. The along-slope currents flowing over topography of small, typically < 10 km, scale on the continental slopes produce internal lee waves with a predominant transfer of momentum towards shallower water, that is up the slope towards and across the shelf break and onto the continental shelf, at least when, in summer, stratification permits their propagation. Analytical results show that even when the lee waves at generation have a component of their group velocity directed towards deeper water, reflection at the sloping sea bed may lead to a turning towards shallower water. A numerical model is used to examine internal wave propagation and to quantify the flux of their momentum across the shelf break. The flux is usually dominated by the larger currents, greater stratification and rougher topography near the top of the slope, and, in conditions in which $f/N \ll 1$, is parameterised by a stress (momentum flux per unit vertical area along the shelf break) per unit length down-slope, τ_*, given by $\tau_* = k\rho_0 VNh^2 \cos^4(\beta + \beta_0)$, where ρ_0 is the mean water density, V is the mean along-slope flow over the slope, N is the buoyancy frequency in the vicinity of the shelf break, f is the Coriolis parameter, and h^2 and β are the mean square amplitude of the topography of wave number, l, such that $Vl/N < 1$, and its mean orientation relative to the upslope direction, respectively. The constant β_0 is $7 \pm 2°$and estimates are for $\beta <$ about 60°. A working value of k of about $(9 \pm 4) \times 10^{-6}$ m^{-2} is suggested, with values near 1.3×10^{-5} m^{-2} when the topography is dominated by wavelengths less than $4\pi V/N$, or 5×10^{-6} m^{-2} when they exceed $20V/N$. This flux represents a transfer of momentum to the shelf currents in a direction contrary to the current over the slope leading to the generation of the internal waves. Time-scales of about 5 days are associated with this transfer on 5° slopes with 10-m-high topography when $N \approx 10^{-2}$ s^{-1}.

1. Introduction

The continental slopes are major topographic features of the surface of the solid Earth, being 4-5 km in height and extending for thousands of kilometres. They have great importance for the oceans. They are sites of upwelling, major fisheries, and generally a maximum (near 1 km depth) in biodiversity. They act as the natural boundaries for the circulation of waters deeper than about 200 m (or more generally, the depth of the shelf-break) and they form the outer boundary of shelf-sea circulations. They are zones of exchange between the shelf seas and the deep ocean of water, particles and solutes, some of anthropogenic origin derived from land. Visual observations show in conditions of summer stratification the shelf break and slopes are often regions of intense internal wave activity (Apel et al., 1975; Baines, 1981; Fedorov and Ginzberg, 1986) and therefore sites at which, if anywhere in the surface ocean, internal wave effects on momentum flux may be significant.

In some areas the tidal streams are directed with large components normal to the shelf break (or across the slope) and generate internal waves and soliton packets as explained, for example, by Maxworthy (1979; see also Hibiya, 1986, 1988; Huthnance, 1989; Lamb, 1994; Gerkema, 1994), but this is not generally the case, and the *mean* currents near the slope at depths greater than that of the shelf break are constrained by stratification and the Earth's rotation to flow approximately along isobaths. Many of the theoretical investigations cited ignore the variation of the continental slope along its length and assume two-dimensionality, whereas inspection of high resolution bathymetric charts of the continental slopes show them to be highly convoluted along their length, being cut by channels, rills, gullies and canyons of a variety of scales; below the shelf break the major variation in small-scale topography is generally in the along-slope direction and so the features lie normal to the mean current direction.

Interaction between the mean along-slope flow and topography generates internal waves and hence a transfer of momentum into the internal wave field (Bretherton, 1969). In the deep ocean the momentum associated with these waves is generally small; they are constrained to lie in a wavenumber band between f/U and N/U, where f is the Coriolis parameter, N is the buoyancy frequency, and U is the current speed, and this band is narrow since N/f is not large. Bell (1975) shows that it is indeed only small, about 300 m horizontal scale, topography, which is effective in generating internal waves in the deep ocean. However, as pointed out by Holloway (1992), N/f is relatively large in the upper ocean and, where topographic variability is large, as near the shelf break, internal wave drag may be important.

This paper describes the transfer of momentum onto a continental shelf by internal waves generated by flow over the slope. It builds on an observation (Thorpe, 1992; see section 2.1 below) that the energy associated with internal

lee waves produced by flow along sloping topography has a bias toward shallow water, being carried by a preferentially positive component of group velocity up the slope and into shallower water, rather than towards deeper water, provided that the characteristics of the water mass allow for internal wave propagation to continue in this direction. This earlier work was based on analytical studies of waves in an infinitely deep ocean and in a fluid with a uniform and steady along-slope flow, V, and uniform buoyancy frequency, N, so that waves of any vertical scale could be generated, propagation was in straight rays, with the effects of surface reflection and subsequent bottom reflections largely ignored. We emphasise that, although concerned primarily with wave *generation* by the along-slope current, the full problem now to be addressed includes the possible subsequent *reflection* of waves from the sea bed, and in principle all the complexity of that much studied problem (see references above). Further progress by analytical methods appears unlikely to be very productive and therefore we have resorted instead to numerical studies (sections 3 and 4) guided by further analysis (section 2), with the overall objective of deriving a parametric description of internal wave drag which might prove useful in numerical models of ocean or shelf-sea circulation.

Such modelling of internal wave momentum transport and breaking in the *atmosphere* is relatively commonplace (see for example, McFarlane, 1987); internal wave drag is now recognised as having a large effect on the circulation (see for example Lilly, 1972; Palmer et al., 1986; Miller et al., 1989; Hoinka and Clark, 1991; Clark and Miller, 1991). In the oceans, the drag contributes to the *lateral* boundary condition which should be applied to models of ocean circulation abutting the continental slopes; we are concerned with both the vertical flux of horizontal momentum *and* in the horizontal flux of horizontal momentum. In this examination of the effects of internal waves we shall only begin to probe the problem of describing the boundary conditions; a full solution demands study both near the boundary itself (where the waves are generated) and in the presently less-well-known regions where waves are dissipated. Our modest objective is to characterise the possible magnitude of the flux rather than to attempt to derive a formulation valid for all slopes, stratification, and flow structures. After all, if the flux is negligible there is little sense in estimating its destination. The parameterisation (see section 4) may require more observations at sea.

The need to correctly describe the lateral boundary conditions on the velocity field in ocean circulation models is discussed by Ierley (1990); he stresses that the choice of conditions is particularly important because of the effect which they may have on the conservation (or otherwise) of potential vorticity.

2. Analytical Results

2.1. The Generation of Internal Lee Waves on a Slope

Internal waves can be generated by the flow over topography on a slope. For simplicity we consider a uniform and steady flow, V, of a fluid with constant buoyancy frequency, N, parallel to the mean isobaths of a uniform slope, which is tilted at angle α to the horizontal and covered by corrugations of wavelength $\lambda = 2\pi/l$ running down the slope at an angle β to the line of maximum slope (Fig. 1), adopting the approach that any topography may be decomposed into Fourier components and a *linear* wave field found by summation. The inclination of an internal wave constant phase surface to the horizontal is given by

$$\theta = \sin^{-1}(\sigma/N), \tag{1}$$

and phase of the waves is stationary if the intrinsic frequency of the waves, σ, satisfies $\sigma/l = Vc_\beta$, so that

$$\theta = \sin^{-1}(\chi c_\beta), \tag{2}$$

where $\chi = Vl/N$ is a Froude number of the flow, such that

$$\left[ps_\alpha^2 + (1-p)c_\beta^{-2}\right]^{1/2} < \chi < c_\beta^{-1}, \tag{3}$$

where $p = 1 - (f/N)^2$ (Thorpe, 1992; here $c_\beta = \cos\beta$ etc.). This may be written $2\pi V/N < \lambda_y < 2\pi V/(N\,[ps_\alpha{}^2 + (1 - p)\,c_\beta{}^{-2}]^{1/2})$, where λ_y is the wavelength of the topography measured along the slope in the y-direction. This implies that even though N may be small in deep water, the values of λ_y for which internal waves will be

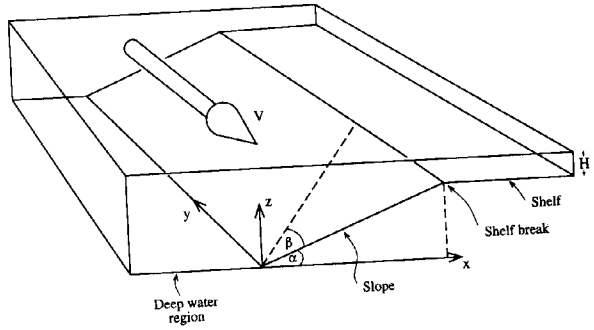

Figure 1. Sketch of the model geometry. The deep water region is generally taken to be 1000 m deep and the shelf 200 m deep. Both are bounded by vertical walls (or by 'spongy layers' to absorb wave energy). Topography is superimposed on the slope (shown 'stippled'). The model is periodic in the along-slope direction. The mean flow is parallel to the line of the shelf break and uniform across the channel formed between the side walls. In section 2 the effect is considered of 'ripples' with crests aligned at angle β as shown.

generated in the ocean are generally limited to scales between about 100 m and 10 km. We find that that waves generated near the upper part of the slope are most effective in the transport of momentum. The Burger number, B = NH/fL, where H is the water depth, is large there and generally it is justified to take $(f/N)^2 << s_\alpha^2 << 1$ (see also caption to Fig. 2). Then (3) becomes

$$s_a < \chi < c_\beta^{-1}. \tag{4}$$

(This can be written $s_\alpha c_\beta < V_1 l/N < 1$, where V_1 is the component of V normal to the crest lines of the topography, a more general form of eq. (4) when the direction of V is in any direction parallel to the plane of the slope). Although the wave phase is stationary in the flow, wave energy propagates with a positive component of group velocity towards shallow water when

$$-\left|\cos^{-1}(s_\alpha/\chi)\right| < \beta < \beta_{crit}, \tag{5}$$

where β_{crit} is the positive root of $c_\beta c_a = \left(1-s_\alpha^2/\chi^2\right)^{1/2}$. There is a preferential trend towards shallow water for moderate values of β; the area of the χ - β plane (Fig. 2) is dominated by propagation towards shallow water. The bias increases as χ decreases from $c_{\beta^{-1}}$ (when $\beta_{crit} = 0$) to s_α (when $\beta_{crit} = \pi/2$ and all waves generated with stationary phase travel towards shallow water whatever the value of β). It is found by simple geometry that the angle between the projection of the relative wave group velocity vector onto the horizontal plane and a horizontal direction pointing upslope normal to the isobaths is ϕ given by

$$\cos\phi = \left[s_\alpha c_\alpha - t_\beta \left(t_\theta^2 c_\alpha^2 + t_\theta^2 t_\beta^2 - s_\alpha^2 \right)^{1/2} \right] / \left[t_\theta \left(c_\alpha^2 + t_\beta^2 \right) \right] \tag{6}$$

(e.g., see Eriksen, 1982; Gilbert, 1990).

2.2. Reflection of Internal Waves at the Sea Surface and Slope; N and α Uniform

The ocean, unlike the atmosphere, has an upper boundary, the sea surface. Reflection of waves from a smooth sea surface or from a smooth slope will preserve the wave frequency and along-slope wavenumber and waves will therefore remain stationary in the along-slope flow.

After downward reflection at the sea surface, waves will return to the sea bed. Provided that $\theta > \alpha$, the angle ϕ will decrease towards zero at each successive reflection of the waves from the slope, even if the internal waves are *generated* with a positive component of their group velocity directed towards deeper water (see Eriksen, 1982, figure 2b). The internal lee waves are therefore *trapped* within the slope-shelf region when $\theta > \alpha$, their group velocity relative to the mean flow progressively turning towards the up-slope direction on each reflection from the bottom. The only waves to escape will be either those generated with a component of group velocity towards deeper water, the areas which are not stippled in Figure 2, or those which, on generation, propagate towards shallow water but have $\theta > \alpha$ (those in the area in Fig. 2 with $\beta > 0$ and $s_\alpha < \chi < s_\alpha/c_\beta$). The latter reflect towards deeper water on their first reflection from the slope. Of the former there are two classes: those which propagate at an angle below the horizontal, which may not intersect the slope, and those which, after their first reflection from the sea

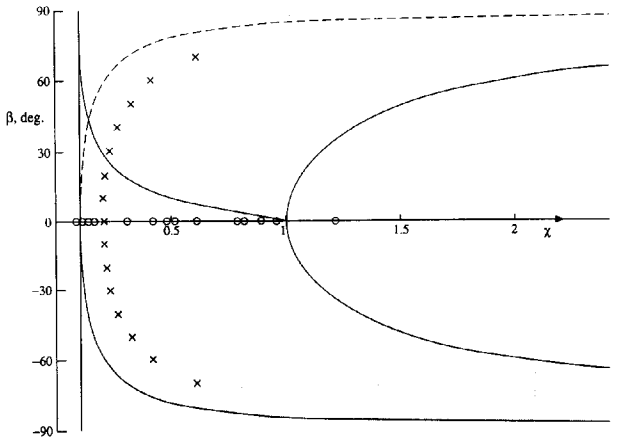

Figure 2. The β - χ plane for $\sin^{-1}\alpha = 0.1$ showing the areas, $s_\alpha < \chi < c^{-1}{}_\beta$, in which stationary phase waves can be formed over sinusoidal topography on a slope. The direction of group propagation of these waves is towards shallow water in the stippled area. This area is bounded by the curve $\beta = \beta_{crit} = \cos^{-1}[(1-s_\alpha^2/\chi^2)^{1/2}/c_\alpha]$ when $\beta > 0$, and by the curve $\chi = s_\alpha/c_\beta$ when $\beta < 0$. The value of θ is $\pi/2$ (vertically propagating waves) on $\chi = c^{-1}{}_\beta$. $\theta = \tan^{-1}(s_\alpha/t_\beta)$ on the full curve separating the areas of different propagation directions for $\beta > 0$. $\theta = \alpha$ on the dashed curve where $\beta > 0$ and on the curve separating directions for $\beta < 0$. Between the latter and $\chi = s_\alpha$ wave propagation is below the horizontal and towards deeper water. On $\chi = s_\alpha$ $\theta = \sin^{-1}(s_\alpha c_\beta)$ and so is less than α. All waves in the sector $s_\alpha/c_\beta < \chi < c^{-1}{}_\beta$ will (after sufficient reflections if $\beta > 0$) propagate towards shallower water depths (see 2.2). The effect of non-negligible f/N is to increase the lower values of χ to $(s_\alpha^2 + f^2/N^2)^{1/2}$. The lower bound of χ increases with increasing $|\beta|$, and the curve separating the regions of wave propagation towards deeper or shallower water in $\beta > 0$ has increasing values of χ at large β. The overall effect is to reduce the area of the χ - β plane in which stationary waves are possible. Crosses and circles correspond to the parameter values at which numerical experiments are made (see Figs. 4 and 5).

surface or on a subsequent group velocity towards deeper water, reach the abyssal plain. (Some waves generated sufficiently near the foot of the slope will always "escape" in this way). Over the area in the χ - β plane in which $s_\alpha/c_\beta < \chi < c_\beta^{-1}$ (Fig. 2) all stationary phase waves, including those which are propagating towards deeper water when generated (provided they reflect sufficiently often from the slope and do not reach the abyssal plain), will eventually propagate towards shallower water depths.

If the the sea surface or slope is rough where the reflection occurs, some of the internal wave energy may be scattered (see Baines, 1971 a,b; Thorpe, 1992) or, for surface reflection, the internal waves may even interact resonantly with the surface waves. For simplicity, these latter effects are disregarded here but should be considered when it comes to comparison of theoretical estimates with observations.

2.3 Effects of Non-Uniform N and α

The conclusions of section 2.2 ignore the variations of N and α which occur in the ocean. Waves propagating upwards towards the sea surface from the lower parts of the slope will encounter regions where the density gradient and therefore N increases. Since the intrinsic frequency, σ, is conserved, the angle of the group velocity vector to the horizontal, $\theta = \sin^{-1}(\sigma/N)$, decreases as N increases, and the wave paths will be refracted towards the horizontal. Since generally α increases towards the shelf break, the waves propagating towards shallower water may therefore return to meet the slope (i.e., propagating at an angle, θ, which is smaller than the local slope), and generally be reflected back toward deeper water. Waves propagating towards deeper water at generation may never reach the surface and will therefore not be reflected back to the slope, will continue to radiate into deeper water, and will not be trapped in the shelf region.

In contrast, If N becomes very small at some depth level below that of the shelf break, as for example, it will do when the depth of the winter convectively mixed layer exceeds that of the continental shelf, internal waves will be unable to propagate beyond the level at which $\sigma = N$ and will be reflected down to be trapped in the wedge between the slope and the level at which $\sigma = N$, possibly with enhanced amplitudes and breaking which may serve to contribute to the further deepening of the convective layer if dissipation is not sufficient to limit them. No momentum will then be carried by the waves onto the shelf.

3. Numerical Results

3.1 The Model

We used a semi-spectral hydrostatic primitive equation model developed by Haidvogel and others (see Haidvogel et al., 1991; Chapman and Haidvogel, 1993) to examine stratified uniform flow along a channel with a section consisting of a constant 200-m-depth shelf, slope with angle α generally taken such that $s_\alpha = 0.1$, giving an 8-km length slope, and constant 1 km depth abyssal plain (Fig. 1). The uniform flow runs parallel to the isobaths of the slope and is laterally constrained by parallel vertical boundaries on the shelf and abyssal plain. Periodic conditions were chosen in the along-slope direction. The vertical flow structure is represented through modified Chebyshev polynomials, seven being found adequate when the buoyancy frequency, N, of the fluid is constant in depth, but twenty-one being found necessary to satisfactorily resolve the flow in some runs (Thorpe, 1995) in which N varies with depth. Experiments were made with uniform and oscillatory flows over topography of various kinds on the slope.

Like Chapman and Haidvogel we adopted a free slip boundary condition at the lower and upper (rigid lid) boundary and included only 'horizontal viscosity', usually set to zero. Where necessary, higher viscosity spongy layers were introduced in the vicinity of the lateral boundaries to prevent their affecting the flow over the slope.

3.2 Steady Flow Over 'Bump' Topography

First test runs of the model proved its integrity through its ability to reproduce earlier results of stratified flow around isolated Gaussian topography on a horizontal plane. Figure 3 is an example of the effect of the slope on the perturbation field caused by an along-slope flow with $N = 10^{-3}$ s^{-1} and speed $V = 0.1$ m s^{-1} over an isolated 10 m high Gaussian 'bump' with scale radius 2.1 km at the position marked with a circle. Shown is the along-slope component of the current field at the sea surface 30 hrs after the onset of the flow, when (a) the slope angle is zero and the water depth is 600 m and (b) when the topography is located at 600m water depth, half way up a uniform slope with $s_\alpha = 0.1$ between the 200 m 'shelf' and the 1000-m deep plain. The wave pattern is distorted in the upslope direction. The momentum flux across the 20-km-long shelf break is given by $Fx_1/\rho_0 VN = 1.55\times10^4$ m^3, and this is about six times greater than the momentum flux across the foot of the slope at the same time.

3.2 Steady Flow Over 'Bump' Topography

First test runs of the model proved its integrity through its ability to reproduce earlier results of stratified flow around isolated Gaussian topography on a horizontal plane. Figure 3 is an example of the effect of the slope on the perturbation field caused by an along-slope flow with $N = 10^{-3}$ s^{-1} and speed $V = 0.1$ m s^{-1} over an isolated 10-m-high Gaussian 'bump' with scale radius 2.1 km at the position marked with a circle. Shown is the along-slope component of the current field at the sea surface 30 hrs after the onset of the flow, when (a) the slope angle is zero and the water depth is 600 m and (b) when the topography is located at 600 m water depth, halfway up a uniform slope with $s_\alpha = 0.1$ between the 200 m 'shelf' and the 1000-m-deep plain. The wave pattern is distorted in the upslope direction. The momentum flux across the 20-km-long shelf break is given by $Fx_1/\rho_0 VN = 1.55 \times 10^4$ m^3, and this is about six times greater than the momentum flux across the foot of the slope at the same time.

3.3 Steady Flow Over Sinusoidal Topography

Further tests of the model were made to establish it produced waves over sinusoidal ripples on the slope at times of about 3-12 hr which were consistent with predictions of the analytical model; their inclinations were in accord with the theory.

Several runs were made to explore the properties of the model with 'typical' values and rippled topography of amplitude a. Seven polynomials were usually taken to define the vertical structure and an along-slope grid of 14 points and an upslope direction grid of 101 point was generally used. Values of the momentum flux through a vertical plane at the shelf break, Fx_1, generally increased with time after the flow was switched on, before settling to a value about which fluctuations of 5-10% occurred after a 'spin-up' time estimated to be approximately equal to that required for waves to arrive from the foot of the slope. Eventual numerical instability proved to be unavoidable with zero viscosity, but was usually delayed until the model had run for some 90 hrs. It was commonly preceded by a fall and then a huge and rapid rise in flux.

The 'steady' momentum flux Fx_1 scales with a^2 as expected by linear theory, at least up to values of $al = 0.024$.

Figure 4 shows the variation of the scaled flux at the shelf break, $F_1 = Fx_1/(a^2\rho_0 VNA)$, where ρ_0 is the mean (reference) density and A is the area of the vertical section at the shelf break, for various values of β and with $V = 0.1$ m s^{-1}, $a = 0.5$ m, $\lambda_y = 3$ km and $N = 1\text{x}10^{-3}$ s^{-1} (the corresponding χ and β values are shown by crosses in Figure 2. Values of Fx_1 are factors of (3.4 ± 1.1) greater than those found for $|\beta| \leq 40°$ when $\nu_H = 1$ m^2 s^{-1}, demonstrating the large damping produced by viscosity when it is included in the numerical model). Slightly higher fluxes are found for $\beta < 0$ than at the corresponding

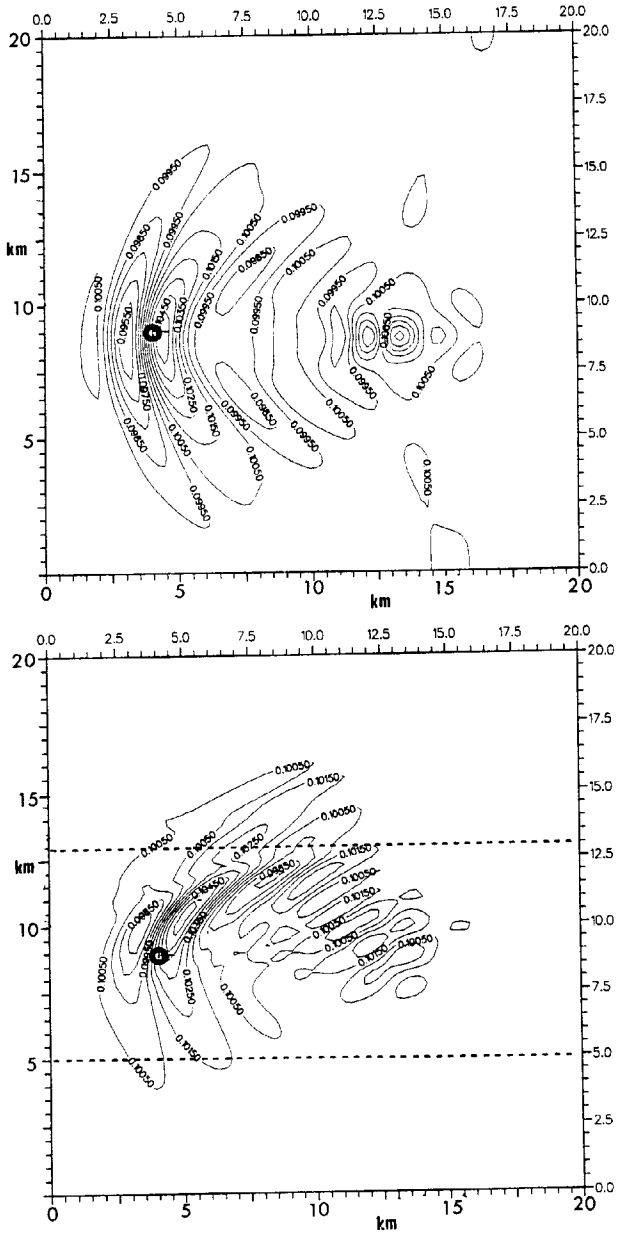

Figure 3. The effect of the slope on the perturbation field caused by an along-slope flow over an isolated 10-m-high Gaussian 'bump' with scale radius 2.1 km at the position marked with a circle. Here $N = 10^{-3}$ s^{-1} and the flow $V = 0.1$ m s^{-1} is to the right. The scales are in km. (a) shows the along-slope component of the current field at the sea surface 30 hr after the onset of the flow, with zero slope angle and 600 m uniform water depth. (b) shows the same current component at the same time when the topography is located at 600 m water depth, but now half way up a uniform slope marked by dashed lines with $s_\alpha = 0.1$ and which lies between the 200 m 'shelf' (at the top) and the 1000-m-deep plain (at the bottom of the figure). Contours are shown at 0.05 cm s^{-1} intervals. The largest current component fluctuation from the mean 10 cm s^{-1} current is 0.45 cm s^{-1}. The effect of the slope is to distort the wave pattern in the upslope direction towards and across the shelf break.

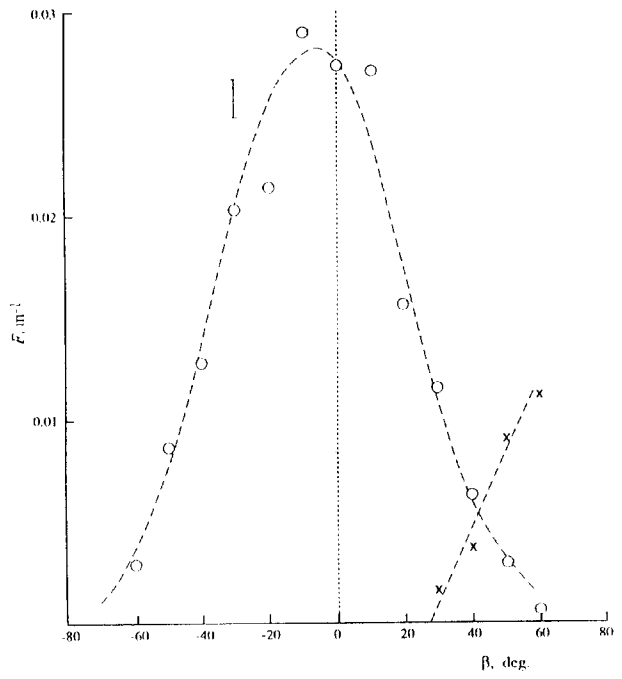

Figure 4. Plot of values of the scaled horizontal flux of horizontal momentum, $F_1 = Fx_1/(a^2\rho_0 VNA)$ (circles) and $F_2 = Fx_2/(a^2\rho_0 VNA)$ (crosses) vs β, derived from the numerical model with values of V = 0.1 m s^{-1}, α = 5.74°, N = 10^{-3} s^{-1}. Larger values of the flux, F_1, are found at negative values of β than at the corresponding positive values. F_2 is significantly greater than zero only when β is greater than about 28° and dominates the flux from the slope when β > 40°. The dashed curve is $F_1 = 0.028 \cos^4(\beta + 7.0°)$.

positive values of β, as expected from the analytical results. The dashed curve in Figure 4 is the best fit of $F_1 = F_{10} \cos^q(\beta + \beta_1)$ to the data having $q = 3.9 \pm 0.15$ and $\beta_1 = 7 \pm 2°$. This figure also shows the scaled horizontal momentum flux through a vertical plane at the foot of the slope, F_2. The value of β_{crit} at which the infinite depth analytical model predicts that the direction of the wave flux changes direction from being towards shallower water depths ($\beta < \beta_{crit}$) to being towards deeper water, is 27.9°. F_2 is negligible for $\beta < \beta_{crit}$ (when all wave propagation is towards shallow water) but increases for larger β, becoming equal to F_1 at β = 42° and exceeding F_1 at larger β. F_1, however, does not approach zero as β increases towards β_{crit}, supporting our earlier conclusion that even when the group velocity of the generated waves has a positive component towards deeper water, reflections from the sea bed will lead to momentum transfer towards shallow water.

Figure 5 shows the variation of the scaled flux, F_1, with χ, when β = 0 and with a = 0.5 m and with V taking values from 0.07 to 0.2 m s^{-1}, N values from 0.5 × 10^{-3} s^{-1} to 2 × 10^{-3} s^{-1}, and λ_y values from 0.5 to 6 km. The mean flux is estimated between 48 and 84 hr after the onset of the flow. At values of χ = 0.105 (close to $\chi = s_\alpha$, when waves propagate with θ close to α) and at 0.90 and 0.97 (near $\chi = c_\beta^{-1}$ when θ is close to π/2) the values of F_1 were unsteady and still generally increasing when numerical instability occurred. Very small values of flux are found when χ > 1. The mean values of the scaled flux are about 0.035, with a rise in values occurring near χ = 0.44. At time t such that Nt = 64.8 (18 hr if N = 10^{-3} s^{-1}) F_1 has reached about half the 'steady' value when 0.1 < χ < 0.3, but is already within the uncertainty of the 'steady' values when 0.5 < χ < 0.8. Over the limited range of values tested, the scaling gives consistent results, at least within the uncertainty of the variations of the estimates, and are independent of λ_y except in so far as it affects χ. As expected, the momentum flux into deep water at the foot of the slope was very small, but positive, for all values of χ. When s_α = 0.2, similar values of F_1 are found near χ = 0.3, but values 50% lower than those shown in Figure 5 when χ = 0.48 and 0.62, suggesting that here at least the flux is proportional to the area of slope generating the waves. F_1 must be zero at α = 0, β = 0.

The magnitude of the stress at the shelf break can be compared to that on the sea bed

$$\tau_B = C_D \rho_0 V^2, \qquad (7)$$

where C_D is a drag coefficient, approximately equal to 3×10^{-3} (Heathershaw, 1979). The maximum momentum flux across the shelf break per unit area when β = 0 is 5 × 10^{-2} $\rho_0 a^2 VN$, which is equal to τ_B (with V = 0.1 m s^{-1}, N = 1

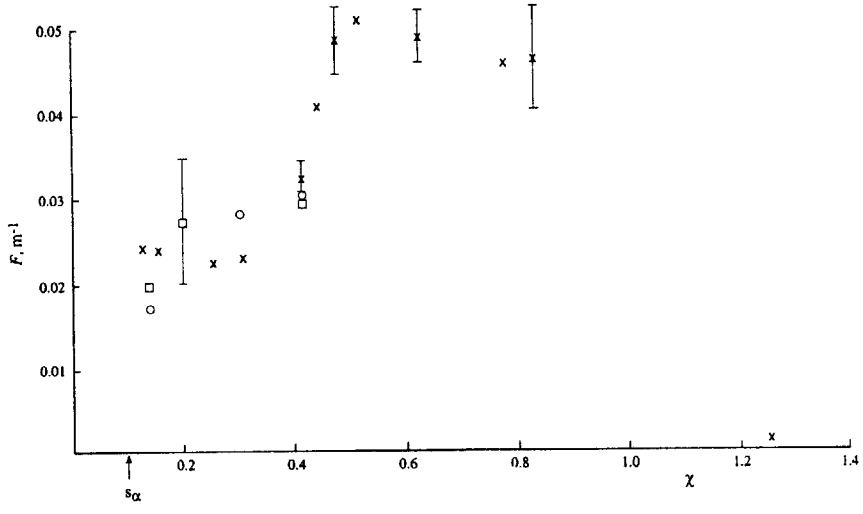

Figure 5. Plot of values of the scaled horizontal flux of horizontal momentum across the shelf break, $F_1 = Fx_1/(a^2\rho_0 VNA)$, versus χ at s_α = 0.1 and β = 0. The points represent variation of (crosses) λ, (circles) U, and (squares) N, from 'typical' values, λ = 3 km, U = 0.1 m s^{-1}, and N = 1×10^{-3} s^{-1}. The vertical bars represent the range of variability of the numerical estimates.

$\times 10^{-3}$ s^{-1}) when a = 2.5 m. This is a small value. The *net* stress in the 200-m-deep water at the shelf break is equal to that on the 8-km sloping boundary when a = 15.5 m, which is not untypical of the amplitude of the real topography on continental slopes. Smaller corresponding values of a would be found if N were larger.

Flow over model 'canyons' is found to produce wave patterns propagating onto the 'shelf', with intensification of currents near the canyon head.

3.4 Other Cases

The effect of flow oscillation and stratification is found to modify the area of the slope and the time over which wave generation is possible, and to create an oscillatory flux. Even a relatively small mean flow can result in a rectified momentum flux of mean magnitude similar to those found in steady flows alone. An area of real topography with mean bottom slope close to 5° and with superimposed topography with relative rms amplitude, h, of 9.2 m has also been modelled. Stress values within the range of those in Figure 5 were found.

4. Discussion

4.1 A Working Value for the Flux Across the Shelf Break

As a working scheme for parameterising the drag coupling between the deep water circulation and the shelf water circulation at the shelf break, the model results described above and comparison with the parameterisation of wave drag in the atmosphere (Thorpe, 1995) suggest a stress τ_* at the shelf break produced by waves generated per unit area of the slope given by

$$\tau_* = k\rho_0 VNh^2\cos^4(\beta + \beta_0), \qquad (8)$$

where ρ_0 is the mean water density, V is the mean along-slope flow over the slope, N is the buoyancy frequency in the vicinity of the shelf break, and h and β are the rms amplitude of the topography of scale such that $\chi < 1$, and its mean orientation respectively. The β variation is derived from Figure 4 with $\beta_0 = 7 \pm 2°$and is probably valid only when $\beta < 60°$. The value k determined from Figure 5 is about 9×10^{-6} m^{-2}, with values near 1.3×10^{-5} m^{-2} when the topography is dominated by wavelengths less than $4\pi V/N$ ($\chi > 0.5$), or 5×10^{-6} m^{-2} when they exceed $20V/N$ ($\chi < 0.3$).

4.2 Is the Momentum Flux Significant?

Equation (8) provides an outer boundary condition for the shelf circulation. Where the momentum is surrendered to the shelf-sea circulation will depend upon the processes which lead to the transfer of stress from the waves, such as wave breaking or wave-flow interaction, and corresponding distances over which these are effective. Internal waves near the shelf break frequently appear as soliton packets which, in a shallow thermocline or water depth, evolve from localised, often single crest or trough, tidal disturbances (Gerkema, 1994). In reality, the waves generated in our models may evolve in a similar fashion. The course resolution of the numerical model fails to show this evolution. Sandstrom and Elliott (1984) observed that internal tidal waves and associated wave solitons are dissipated within about 10 km of the shelf break and over periods of about 5×10^4 s, with shear flow instability probably playing a part. In their analysis of other observations of internal waves propagating on the shelf, Sanford and Grant (1987) conclude that dissipation in the benthic boundary layer is unable to account for the dissipation observed; other mechanisms must be important.

We may estimate an eddy diffusion coefficient for momentum at the shelf break, κ, from the equation $\tau/\rho_0 = \kappa\, dU/dx$. If we write $dU/dx = U/\mathrm{Ro}$, where Ro is the internal Rossby radius of deformation of the shelf waters (equal to NH/f) and which we might suppose provides a scale for wave-flow momentum transfer (arguably the scale might increase with H and f^{-1}, and decrease when stratification decays in winter), then with $\tau = \tau_*$, $\kappa = k N^2h^2H/f$, so that the coefficient scales with h^2, the mean square roughness of the topography on the slope. The value of κ falls to zero when N tends to zero, a condition (as in winter) in which no internal waves can propagate onto the shelf. With $N = 10^{-3}$ s^{-1}, $f = 10^{-4}$ s^{-1}, H = 200 m and h = 10 m, $\kappa = (14 \pm 6) \times 10^2$ m^2 s^{-1}, a large value at the scale, 20 km, of the corresponding Ro (less than the 10 km found by Sandstrom and Elliott, 1984).

We may alternatively estimate a time-scale associated with the rate of transport across the shelf break, the ratio of the momentum in the slope current divided by the flux. The momentum per unit along-slope length of the current is its cross-sectional area multiplied by $V\rho_0$ and, using the $s_\alpha = 0.1$ slope from 200 m depth to 1000 m depth, this is $9.6 \times 10^6\, V\rho_0$ (SI units). The corresponding momentum flux is $\tau_* x$ (200 m) × (8 km), and the time scale is $1.2 \times 10^4/kNa^2$, or (4.9 ± 2.1) days if $N = 10^{-2}$ s^{-1}. This is sufficiently small for the flux to be a significant factor in the balance of forces driving and dissipating the flows.

The wave momentum is positive in the direction of wave propagation through the mean flow, and therefore has a positive component in a direction *contrary* to the mean flow which is supported by the pressure acting on the sea bed. The momentum transferred back into the mean flow when waves break, or otherwise interact with the flow field to transfer their momentum to it, will therefore accelerate the fluid in a direction contrary to the mean flow over the slope generating area, retarding the mean current where it is in the slope flow direction or possibly driving a counter current on the shelf. Since the internal waves reaching the shelf have a component of

momentum directed in the on-shelf direction, the source of which is a component of the lift forces experienced by the topography, they may also tend to drive flow onto the shelf, at least until resisted by the production of adverse pressure gradients from the shoreward boundary.

Acknowledgement. Jiang and Keen had funding from NERC Grant GR3/8001 and Keen received funding from the EEC MAST II OMEX programme MAS2 CT93-0069. We are grateful for the support provided.

References

Apel, J.R., H.M. Byrne, J.R. Proni, and R.J. Charnell, 1975: Observations of oceanic internal and surface waves from the Earth Technology Resources Satellite. *J. Geophys. Res.* 80, 865-881.

Baines, P.G., 1971a: The reflection of internal/inertial waves from bumpy surfaces. *J. Fluid Mech.*, 46, 273-291.

Baines, P.G., 1971b: The reflection of internal/inertial waves from bumpy surfaces: Part 2. Split reflection and diffraction. *J. Fluid Mech.*, 49, 113-131.

Baines, P.G., 1981: Satellite observations of internal waves on the Australian north-west shelf. *Aust. J. Mar. Freshwater Res.* 32, 457-463.

Bell, T.H., 1975: Topographically generated internal waves in the open ocean. *J. Geophys. Res.*, 80, 320-327.

Bretherton, F.P., 1969: Momentum flux by gravity waves. *Q. J. R. Meteorol. Soc.*, 95, 213-243.

Chapman, D.C., and D.B. Haidvogel, 1993: Generation of internal lee waves trapped over a tall isolated seamount. *Geophys. Astrophys. Fluid Dyn.*, 69, 33-54.

Clark, T.L., and M.J. Miller, 1991: Pressure drag and momentum fluxes due to the Alps. II: Representation in large-scale atmospheric models. *Q. J. R. Meteorol. Soc.* 117, 527-552.

Eriksen, C.C., 1982: Observations of internal wave reflection off sloping bottoms. *J. Geophys. Res.* 87, 525-538.

Fedorov, K.N., and A.I. Ginzberg, 1986: Visually observed sea surface phenomena. *Oceanology*, 26, 1-7.

Gerkema, T., 1944: Nonlinear dispersive internal tides: generation models for a rotating ocean. PhD dissertation for the Universiteit Utrecht, 149 pp.

Gilbert, D., 1990: Theory and observation of internal wave reflection off sloping topography. PhD dissertation, Department of Oceanography, Dalhousie University, Nova Scotia, Canada, 180 pp.

Haidvogel, D.B., J.L. Wilkin, and R. Young, 1991: A semi-spectral primitive equation ocean circulation model using vertical sigma and orthogonal curvilinear horizontal coordinates. *J. Comp. Phys.*, 94, 151-185.

Heathershaw, A.D., 1979: The turbulent structure of the bottom boundary layer in a tidal current. *Geophys. J. Roy. Astronom. Soc.* 58, 395-430.

Hibiya. T., 1986: Generation mechanism of internal waves by tidal flow over a sill. *J. Geophys. Res.*, 91, 7697-7708.

Hibiya, T., 1988: The generation of internal waves by tidal flow over Stellwagen Bank. *J. Geophys. Res.*, 93, 533-542.

Hoinka, K.P., and T.L. Clark, 1991: Pressure drag and momentum fluxes due to the Alps. II: Comparison between numerical simulations and observations. *Q. J. R. Meteorol. Soc.* 117, 495-525.

Holloway, G., 1992: Representing topographic stress for large-scale ocean models. *J. Phys. Oceanogr.* 22, 1033-1046.

Huthnance, J.M., 1989: Internal tides and waves near the continental shelf edge. *Geophys. Astrophys. Fluid Dyn.*, 48, 81-106.

Ierley, G.R., 1990: Boundary layers in the general ocean circulation. *Ann. Rev. Fluid Mech.*, 22, 111-142.

Lamb, K.G., 1994: Numerical experiments of internal wave generation by strong tidal flow across a finite amplitude bank edge. *J. Geophys. Res.* 99, 843-864.

Lilly, D.K., 1972: Wave momentum flux - a GARP problem. *Bull. Am. Meteorol. Soc.* 53, 17-23.

Maxworthy, T., 1979: A note on the internal solitary waves produced by tidal flow over a three-dimensional topography. *J. Geophys. Res.* 84, 338-346.

McFarlane, N.A., 1987: The effect of orographically excited gravity wave drag on the general circulation of the lower stratosphere and troposphere. *J. Atmos. Sci.*, 44, 1775-1800.

Miller, M.J., T.N. Palmer, R. Swinbank, 1989: Parametrization and influence of subgridscale orography in general circulation and numerical weather prediction models. *Meteorol. Atmos. Phys.* 40, 84-109.

Palmer, T.N., G.J. Shutts, and R. Swinbank, 1986: Alleviation of a systematic westerly bias in general circulation and numerical weather prediction models through an orographic gravity wave drag parametrisation. *Q. J. R. Met. Soc.* 112 , 1001-1039.

Sandstrom, H., and J.A. Elliott, 1984: Internal tide and solitons on the Scotian Shelf; a nutrient pump at work. *J. Geophys. Res.*, 89, C4, 6415-6426.

Sanford, L.P. and W.D. Grant, 1987: Dissipation of internal wave energy in the bottom boundary layer on the continental shelf. *J. Geophys. Res.*, (C2), 1828-1844.

Thorpe, S.A., 1992: The generation of internal waves by flow over the rough topography of a continental slope. *Proc. R. Soc. Lond. A*, 439, 115-130.

Thorpe, S.A., 1995: The cross-slope transport of momentum by internal waves generated by along-slope currents over topography. Submitted to *JPO*.